Regular Article

INORGANIC CHEMISTRY RESEARCH
Published by the
Iranian Chemical Society
www.inorgchemres.org
info@inorgchemres.org

Inorg. Chem. Res., *Vol. 5, No. 1, 112-119, June 2021*
DOI: 10.22036/icr.2021.262552.1099

Catalytic Properties of Ag@Zn-MOF Nanocomposites for Dehydrogenation of Ammonia Borane

Reza Sacourbaravi, Zeinab Ansari-Asl*, Mohammad Kooti and Valiollah Nobakht

Department of Chemistry, Faculty of Science, Shahid Chamran University of Ahvaz, Ahvaz, Iran

(Received 18 December 2020, Accepted 28 January 2021)

The utilization of NH_3BH_3 (ammonium borane) as a H_2 gas storage compound is restricted by its slow rate for H_2 evolution. In this study, three Ag@Zn-MOF nanocomposites with different amounts of Ag:Zn-MOF ratio of 0.25:1 (1), 0.5:1 (2) and 1:1 (3) were investigated as catalysts for hydrogen evolution from hydrolysis of NH_3BH_3. Well dispersed encapsulated Ag nanoparticles (30-60 nm) in the matrix of the composites have been prepared in the presence of Zn(II) metal-organic frameworks (Zn-MOFs) in an aqueous solution by using $NaBH_4$ as a reducing agent at room temperature. These nanocomposites have shown good catalytic activity for the hydrolysis of NH_3BH_3.

Keywords: Hydrogen generation, Ammonia borane, Metal-organic framework, Nanocatalyst

INTRODUCTION

Effective hydrogen storage materials have attracted much attention in the last decades because hydrogen is considered as a clean energy source owing to its power density, efficiency and less environmental problems [1-3]. Ammonia borane (NH_3BH_3) is an environmentally benign, stable, and nontoxic hydrogen storage compound. It is considered as a suitable hydrogen storage material due to its high hydrogen capacity, predominant stability, and high solubility in aqueous solutions [4,5]. Hydrogen can be released from NH_3BH_3 through hydrolysis or thermolysis routes catalyzed by some heterogeneous or homogenous catalysts such as pure metal nanoparticles (MNPs) and their composites [6,7]. Compared to the thermolysis of NH_3BH_3, the hydrolysis of this compound doesn't generate harmful gases. However, due to the stability of NH_3BH_3 in the solid state and in solution, under ambient conditions, a proper catalyst is required for its hydrolysis [8].

Some metal nanoparticles (MNPs), and more frequent their nanocomposites, are reported as effective heterogeneous catalysts for the dehydrogenation of NH_3BH_3. The distribution of MNPs in the matrix of the composites is considered as a crucial factor in the heterogeneous catalysis These MNPs can be well-dispersed into the pores and channels of porous structures. In this route, the porous compounds provide reaction selectivity and enhance catalytic site stability [9-11].

Recently, metal-organic frameworks (MOFs) have been reported as suitable supports for MNPs owing to their unique structural properties. These chemical materials are crystalline compounds that can be prepared from metal ions and organic linkers. MOFs have interesting characteristics, including diversity, high porosity and high surface area. Therefore, MOFs are considered as promising materials for application in various fields such as biomedicine, catalysis, and gas storage [12-14]. The porous structure of MOFs enables proper dispersion of MNPs in the fabricated nanocomposites, enhancing their catalytic performance [15-17].

The immobilization of different MNPs into the structure of MOFs and fabrication of their heterogeneous nanocomposites are conducted by many researchers.

*Corresponding author. E-mail: z.ansari@scu.ac.ir

Zhu *et al.* used AuNi@MIL-101 as a catalyst for dehydrogenation of NH_3BH_3, and around 70 mL of hydrogen was generated over 2.67 min with a turnover frequency (TOF) value of 66.2 mol H_2.mol cat min^{-1} [18]. Also, Liu and coworkers investigated the hydrolysis of NH_3BH_3 at room temperature and reported that Ru@MIL-101 could catalyze this reaction [19].

In this study, the catalytic activity of Ag@Zn-MOF nanocomposites, made by supporting of Ag NPs on a Zn-MOF [20], for hydrogen generation from the hydrolysis of NH_3BH_3 at different conditions was investigated.

EXPERIMENTAL

Materials and Methods

Sodium borohydride ($NaBH_4$) and ammonium sulfate ($[NH_4]_2SO_4$) were obtained from Merck. Ethanol (EtOH) and tetrahydrofuran (THF) were purchased from Sigma. The FT-IR spectra and PXRD patterns of the synthesized NH_3BH_3 were recorded on a Perkin Elmer spectrum two spectrophotometer and PXRD pattern was obtained from X'Pert PRO powder diffractometer, using CuKα radiation. SEM and TEM images were recorded using TESCAN MIRA3 and LEO 906E microscopes, respectively. The Ag species concentration was assessed by inductively coupled plasma (ICP; AGILENT, ICP-7900) technique.

Preparation of Ag@Zn-MOF Nanocomposites

Ag@Zn-MOF catalysts were prepared *via* the encapsulation of Ag ions into the Zn-MOF structure with a subsequent reduction using $NaBH_4$ as a reducing agent. The detailed process for the preparation and characterization of the Zn-MOF and its Ag NPs impregnated Zn-MOF nanocomposites have been reported in our previous research [20]. In brief, Zn-MOFs were loaded with Ag^+ ions by the suspension of Zn-MOF nanoparticles into a silver nitrate solution. After reducing of Ag^+ ions with sodium borohydride, Ag@Zn-MOF nanocomposites were separated, washed with water, ethanol, and dried in an oven.

Synthesis of NH_3BH_3

Sodium borohydride (1.0 g, 26 mmol) was added to 7.34 g of ammonium sulfate (56 mmol) in 50 mL of THF. After refluxing at 40 °C under a nitrogen atmosphere for 2 h, the mixture was centrifuged. Then, the solvent was evaporated from supernatant under vacuum to obtain NH_3BH_3 as white crystals [21].

Catalytic Performance of Ag@Zn-MOF Nanocomposites in the Dehydrogenation of NH_3BH_3

A mixture of the predetermined amount of Ag@Zn-MOF nanocomposite (10 mg), $NaBH_4$ (5 mg, 0.13 mmol), and NH_3BH_3 (22.5 mg, 0.32 mmol) was placed in a two-necked flask. One neck of the flask was sealed with a rubber stopper and a gas burette was connected to the other neck of the flask. Using a syringe 5 mL of distilled water was introduced into the flask. The reaction started immediately after the first drops of distilled water reached the mixture. The reaction was continuously stirred at room temperature. When gas evolution is stopped this point is considered as the end of a hydrolysis reaction. For recyclability study of the as-prepared nanocomposites, after completion the first experiment, Ag@Zn-MOF nanocomposite was separated by centrifuging and washed with H_2O and EtOH, respectively. Then, the recovered catalyst was used in a new reaction. The catalyst was recycled and used for three times.

RESULTS AND DISCUSSION

Preparation of the Ag@Zn-MOF catalysts was involved incorporating of the Ag^+ ions into the Zn-MOF and reducing these ions using $NaBH_4$ as a reducing agent (Scheme 1). The SEM and TEM images (Fig. 1) confirmed the presence of the incorporated spherical Ag NPs with diameters 30-60 nm into the Zn-MOF matrix. The weight percent of Ag element in the structure of the nanocomposites was quantitatively determined by ICP technique as 1.6, 3.1, and 6.5 % for 1-3, respectively.

The NH_3BH_3 hydrolysis was studied as a model reaction to investigate the catalytic activity of the as-prepared nanocomposites. Four critical factors that can affect the catalytic performance of Ag@Zn-MOF nanocomposites are: Ag NPs to Zn-MOF mass ratio, catalyst amount, volume of solvent, and temperature. The maximum H_2 gas generation can be achieved by determining the proper reaction conditions.

Before starting the study of the catalytic performance of the as-fabricated Zn-MOF in the hydrolysis of NH_3BH_3, a

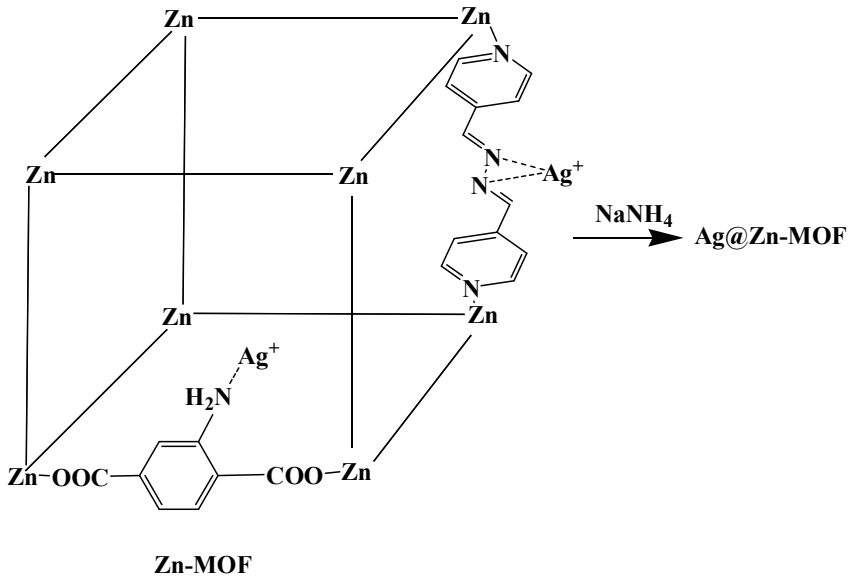

Scheme 1. Schematic illustration of the preparation of Ag@Zn-MOF nanocomposites

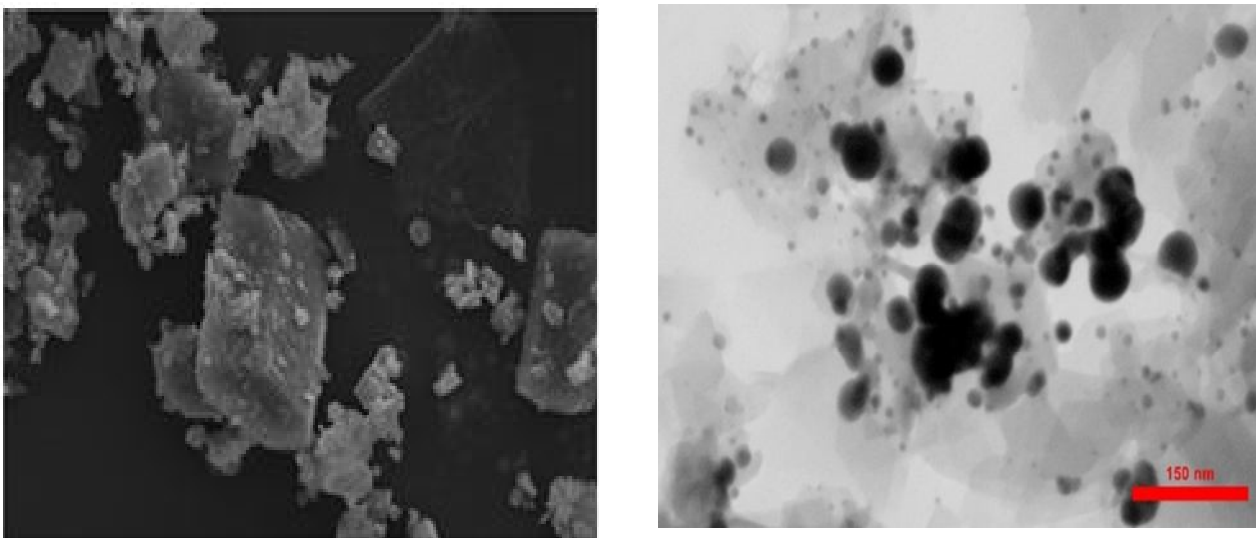

Fig. 1. SEM and TEM images of Ag@Zn-MOF (3) nanocomposite [20].

control test was conducted to find its catalytic property. As reported by Xu *et al.*, an activated complex that formed through the interaction of NH_3BH_3 with the surfaces of the used catalyst was dissociated by attacking water molecules and generated hydrogen gas. The activated complex formation is considered as the rate-determining step [22]. The porous structure of Zn-MOF impregnated with Ag NPs can interact with NH_3BH_3 better than pristine Zn-MOF and therefore Ag NPs facilitate the formation of activated complexes.

$$2\ NaBH_4 + (NH_4)_2SO_4 \xrightarrow{THF} 2\ NH_3BH_3 + Na_2SO_4 + 2\ H_2$$

Scheme 2. Synthesis of the NH_3BH_3

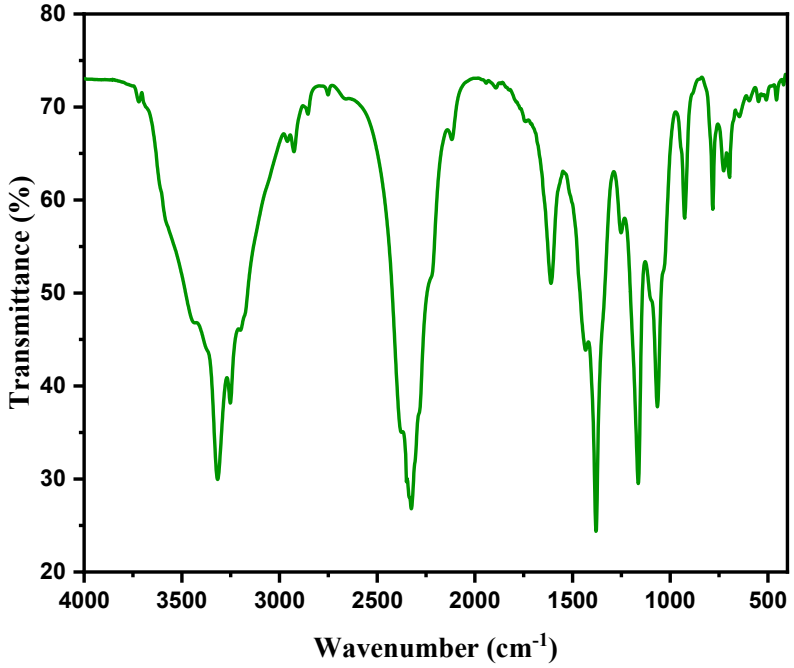

Fig. 2. FT-IR spectrum of NH_3BH_3.

Synthesis and Characterization of NH_3BH_3

NH_3BH_3 was synthesized according to Scheme 2. The FT-IR spectrum of the NH_3BH_3 sample (Fig. 2) is identified by strong absorptions at 3316 and 3251 cm^{-1}, ascribing to the N-H asymmetric and symmetric stretching, respectively. The absorption peak around 2325 cm^{-1} is assigned to ν(B-H). The band attributing to ν(B-N) was observed around 726-782 cm^{-1} [21,23].

The PXRD pattern of NH_3BH_3 (Fig. 3) shows a strong diffraction peak at 2θ = 24° and is in agreement with the previous reports [24,25]. The result indicates high crystallinity of the as-prepared NH_3BH_3.

Catalytic Performance of the As-fabricated Ag@Zn-MOF

Effect of the catalyst with different amount of Ag@Zn-MOF. The catalytic performance of the pure Zn-MOF was tested to compare it with its Ag NPs loaded nanocomposites. According to our study, free Zn-MOF exhibited no catalytic activity in the hydrolysis of NH_3BH_3. This finding indicates the crucial role of Ag NPs in this catalysis reaction.

The dependence of dehydrogenation of NH_3BH_3 on the Ag content of the nanocomposite was investigated using catalysts with fixed amount of NH_3BH_3, $NaBH_4$, and solvent but with different amount of silver. Figure 4 shows the hydrogen volume plots *versus* time for hydrolysis of NH_3BH_3 catalyzed by the Ag@Zn-MOF nanocomposites with different Ag NPs loadings. As it can be clearly seen, the increase of Ag NPs amount in the nanocomposite increases the hydrogen generation, revealing the critical role of Ag NPs as active catalytic sites. Various Ag NPs catalysts have been reported for hydrolytic hydrogen evolution of NH_3BH_3. As appeared in this figure, the generation of 41, 35.5 and

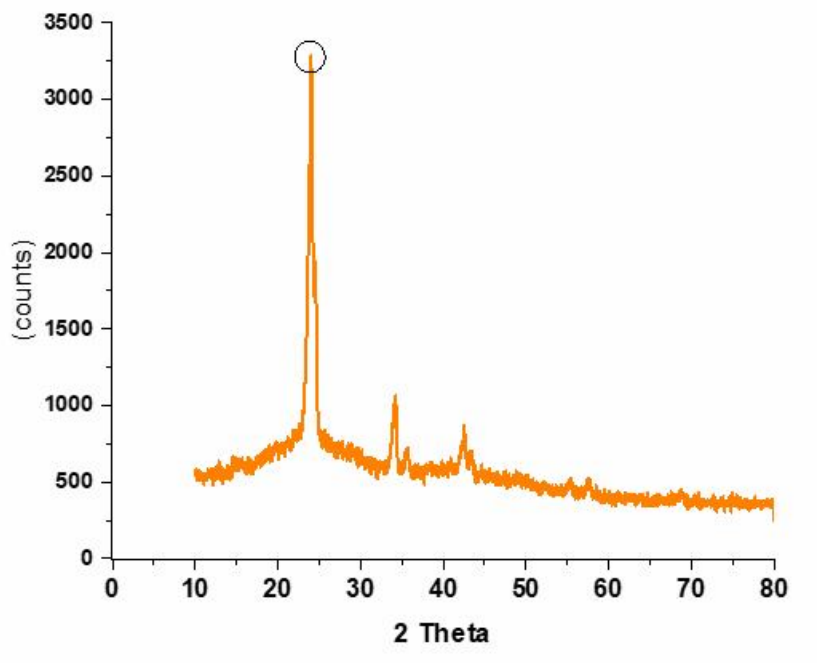

Fig. 3. PXRD pattern of NH_3BH_3.

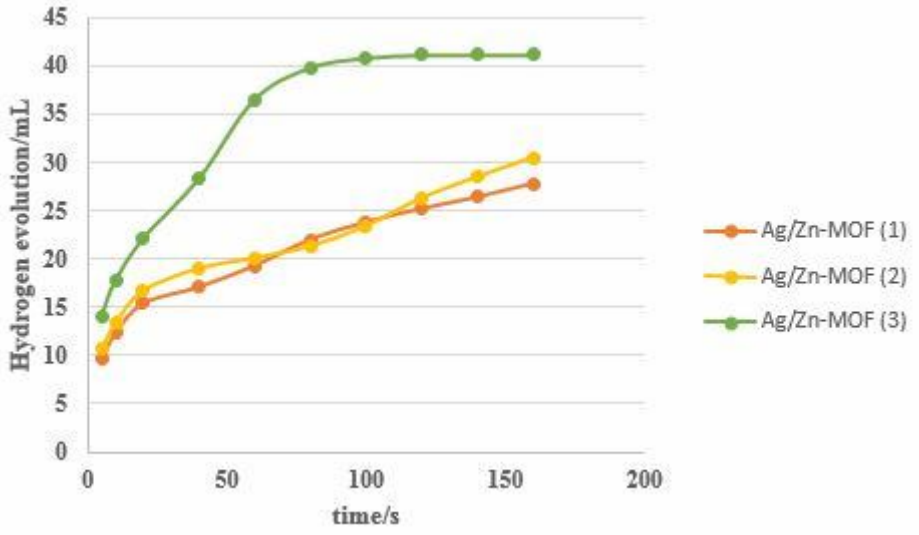

Fig. 4. Hydrogen evolution by the hydrolysis of NH_3BH_3 in the presence of the as-fabricated catalysts.

29 mL of hydrogen was obtained in 120, 220 and 200 min, respectively for Ag@Zn-MOF (3), Ag@Zn-MOF (2), and Ag@Zn-MOF (1) nanocomposites. Owing to the promising catalytic activity of the Ag@Zn-MOF (3) nanocomposite, further investigations were also conducted using this catalyst. In this catalysis reaction, hydrogen gas production

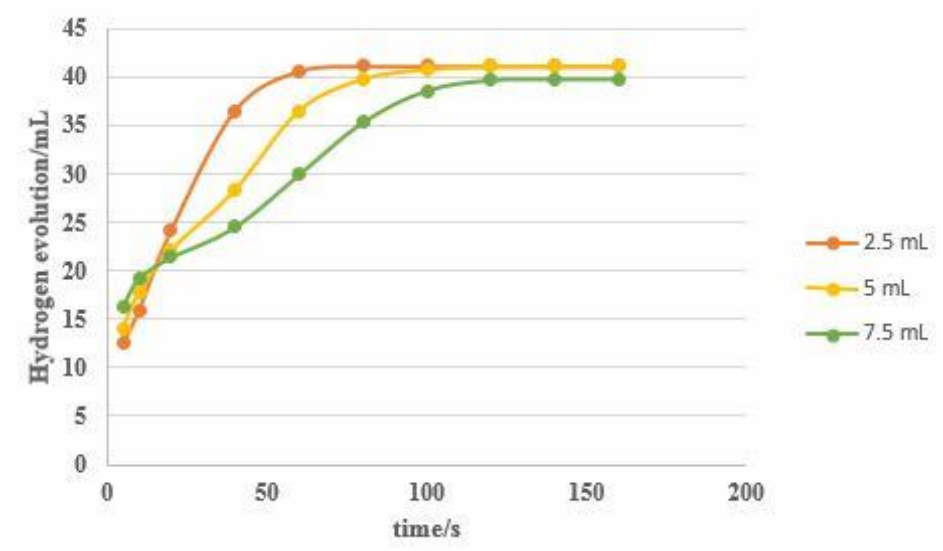

Fig. 5. Hydrogen evolution by the hydrolysis of NH_3BH_3 in the presence of the as-fabricated Ag@Zn-MOF (3) by using different volumes of H_2O as solvent.

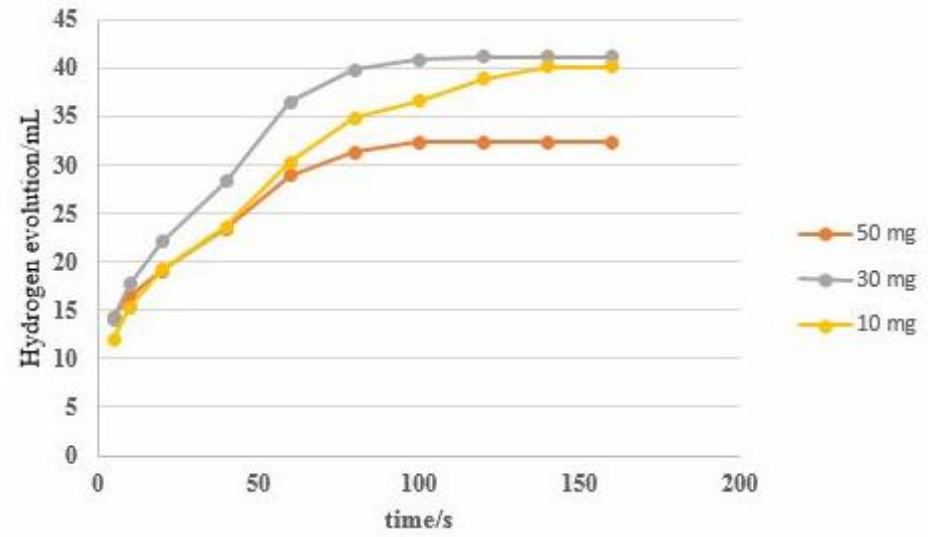

Fig. 6. Hydrogen evolution by hydrolysis of NH_3BH_3 in the presence of the different amounts of Ag@Zn-MOF (3).

is evaluated according to the following equation.

$$NH_3BH_3 + 2H_2O \xrightarrow{Catalyst} 2NH_4^+ + BO_2^- + 3H_2$$

Effect of water volume. To find the optimum conditions, the effect of H_2O volume on the hydrogen evolution was also studied by using different volumes (2.5-7.5 mL), whereas other factors are kept unchanged. The results of three different volumes (2.5, 5 and 7.5 mL) of distilled water on the dehydrogenation of NH_3BH_3 are presented in Fig. 5. It was found that for the conditions as mentioned above, maximum volume for H_2 generation over a

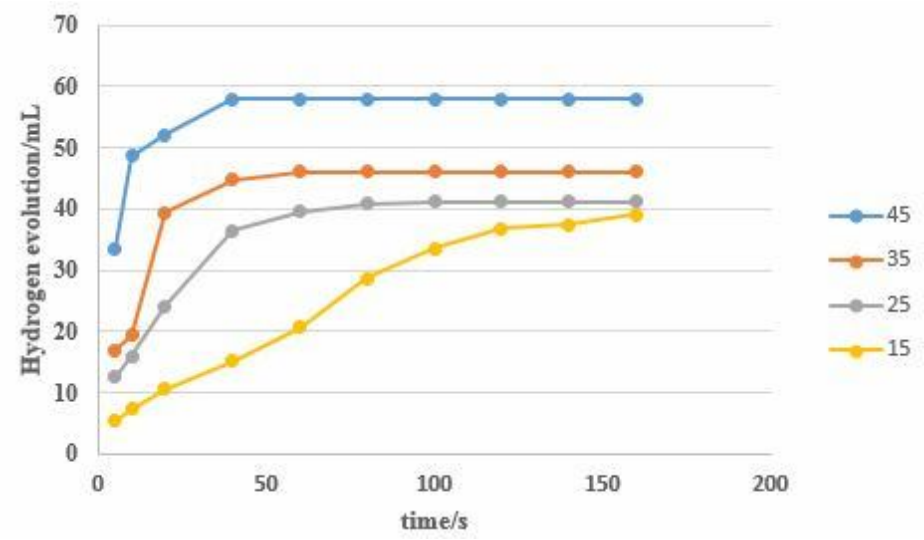

Fig. 7. Hydrogen evolution by the hydrolysis of NH_3BH_3 in the presence of the as-fabricated Ag@Zn-MOF (3) at different temperatures

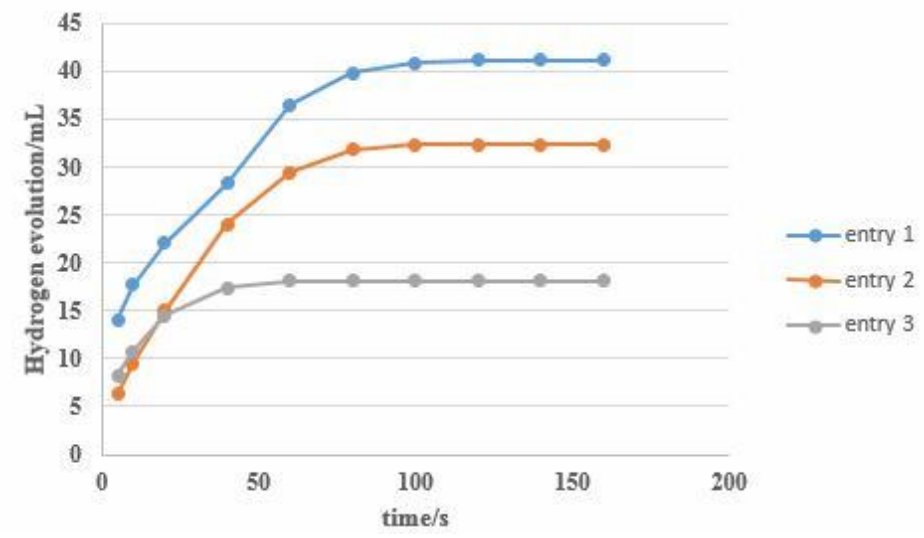

Fig. 8. Hydrogen evolution by the hydrolysis of NH_3BH_3 in the presence of the as-fabricated Ag@Zn-MOF (3).

shorter time was obtained for 2.5 mL of H_2O. This finding indicates that dilution of the hydrogen generator substrates decreases the rate of hydrogen production.

Effect of catalyst dose. Figure 6 exhibits the plot of hydrogen generation versus catalyst amount of the as-fabricated nanocomposite for the catalytic hydrolysis of NH_3BH_3. It was observed that the hydrogen evolution is dependent on the used catalyst amounts. The obtained results indicated an optimum amount of the catalyst exhibits highest activity for NH_3BH_3 hydrolysis. Therefore, the optimum amount of catalyst which is 30 mg was used further study.

Temperature. The effect of temperature has also been studied on the volume of hydrogen (Fig. 7). The amount of catalyst, $NaBH_4$ and H_2O was kept constant. When the

temperature was raised, the volume of hydrogen gas increased. These studies demonstrated that Ag@Zn-MOF nanocomposite has temperature dependent catalytic performance for the dissociation of NH_3BH_3.

Investigation of catalyst recyclability. Recycling studies were conducted under the optimized conditions (2.5 mL H_2O, 30 mg of catalyst, and 45 °C). As it is seen in Fig. 8, the catalytic activity of Ag@Zn-MOF nanocomposite noticeably declines after the second run. This observation indicates that the as-fabricated catalyst more or less loses its activity for the hydrogen generation from hydrolysis of NH_3BH_3 aqueous solutions.

CONCLUSIONS

The catalytic property of various catalysts is generally dependent upon the support, metal particle size, and surface morphology. Zn-MOF is used as a support for Ag NPs (30-60 nm) which were fabricated by reducing of Ag^+ ions loaded onto the Zn-MOF surface. After loading of Ag NPs on the surface of Zn-MOF, its catalytic performance was studied for NH_3BH_3 hydrolysis. The Ag@Zn-MOF nanocomposites showed catalytic activity toward hydrogen evolution *via* hydrolysis of NH_3BH_3. Among the studied nanocomposites 1-3, Ag@Zn-MOF (3) which has the highest content of Ag NPs, shows better activity for hydrogen gas generation.

ACKNOWLEDGEMENTS

The authors gratefully acknowledge the financial support (Grant No.: SCU.SC98.206) from the Shahid Chamran University of Ahvaz, Iran.

REFERENCES

[1] S. Eken Korkut, H. Küçükkeçeci, Ö. Metin, ACS Appl. Mater. Interfaces 12 (2020) 8130.

[2] L. Xu, S. Xiong, S. Zhong, S. Bai, Y. Jiao, J. Chen, Vacuum 174 (2020) 109213.

[3] S. Liu, X. Chen, Z.-J. Wu, X.-C. Zheng, Z.-K. Peng, P. Liu, Int. J. Hydrog. Energy 44 (2019) 23610.

[4] Y.-T. Li, X.-L. Zhang, Z.-K. Peng, P. Liu, X.-C. Zheng, ACS Sustain. Chem. Eng. 8 (2020) 8458.

[5] H. Çelık Kazici, Ş. Yilmaz, T. Şahan, F. Yildiz, Ö.F. Er, H. Kivrak, Front. Energy 14 (2020) 578.

[6] Y. Wu, Y. Sun, W. Fu, X. Meng, M. Zhu, S. Ramakrishna, Y. Dai, ACS Appl. Nano Mater. 3 (2020) 2713.

[7] M. Gao, Y. Yu, W. Yang, J. Li, S. Xu, M. Feng, H. Li, Nanoscale 11 (2019) 3506.

[8] P. Song, Y. Li, W. Li, B. He, J. Yang, X. Li, Int. J. Hydrog. Energy 36 (2011) 10468.

[9] J. Zhang, L. Wang, B. Zhang, H. Zhao, U. Kolb, Y. Zhu, L. Liu, Y. Han, G. Wang, C. Wang, D.S. Su, B.C. Gates, F.-S. Xiao, Nat. Catal. 1 (2018) 540.

[10] A. Zanon, F. Verpoort, Coord. Chem. Rev. 353 (2017) 201.

[11] A. Zhou, Y. Dou, J. Zhou, J.-R. Li, Chem. Sus. Chem. 13 (2020) 205.

[12] W.-G. Cui, G.-Y. Zhang, T.-L. Hu, X.-H. Bu, Coord. Chem. Rev. 387 (2019) 79.

[13] Y. Liu, Y. Zhao, X. Chen, Theranostics 9 (2019) 3122.

[14] H. Li, K. Wang, Y. Sun, C.T. Lollar, J. Li, H.-C. Zhou, Mater. Today 21 (2018) 108.

[15] M. Yadav, Q. Xu, Chem. Commun. 49 (2013) 3327.

[16] Y.K. Park, S.B. Choi, H.J. Nam, D.-Y. Jung, H.C. Ahn, K. Choi, H. Furukawa, J. Kim, Chem. Commun. 46 (2010) 3086.

[17] Y. Zhao, J. Zhang, J. Song, J. Li, J. Liu, T. Wu, P. Zhang, B. Han, Green Chem. 13 (2011) 2078.

[18] Q.-L. Zhu, J. Li, Q. Xu, J. Am. Chem. Soc. 135 (2013) 10210.

[19] T. Liu, Q. Wang, B. Yan, M. Zhao, W. Li, H. Bie, J. Nanomater. 2015 (2015) 679526.

[20] R. Sacourbaravi, Z. Ansari-Asl, M. Kooti, V. Nobakht, E. Darabpour, J. Inorg. Organomet. Polym. Mater. 30 (2020) 4615.

[21] A. Kantürk Figen, M.B. Pişkin, B. Coşkuner, V. İmamoğlu, Int. J. Hydrog. Energy 38 (2013) 16215.

[22] Q. Xu, M. Chandra, J. Power Sources 163 (2006) 364.

[23] J. Huang, Y. Tan, Q. Gu, L. Ouyang, X. Yu, M. Zhu, J. Mater. Chem. A 3 (2015) 5299.

[24] A.K. Figen, M.B. Pişkin, B. Coşkuner, V. İmamoğlu, Int. J. Hydrog. Energy 38 (2013) 16215.

[25] Y.-J. Wu, C.-Y. Wang, ACS Sustain. Chem. Eng. 7 (2019) 16013.